

Origin of Stationary Domain Wall Enhanced Ferroelectric Susceptibility

Shi Liu*

*Extreme Materials Initiative, Geophysical Laboratory,
Carnegie Institution for Science, Washington, D.C. 20015-1305 USA*

R. E. Cohen†

*Extreme Materials Initiative, Geophysical Laboratory,
Carnegie Institution for Science, Washington, D.C. 20015-1305 USA and
Department of Earth- and Environmental Sciences,
Ludwig Maximilians Universität, Munich 80333, Germany*

(Dated: September 29, 2016)

Abstract

Ferroelectrics usually adopt a multi-domain state with domain walls separating domains with polarization axes oriented differently. It has long been recognized that domain walls can dramatically impact the properties of ferroelectric materials. The enhancement of low-field susceptibility/permittivity under subswitching conditions is usually attributed to the reversible domain wall vibration. Recent experiments highlight the stationary domain wall contribution to the dielectric susceptibility irrespective of any lateral displacements or deformations of the wall. We study the effects of domain walls on low-field permittivity of PbTiO_3 with density functional theory and molecular dynamics simulations. The static dielectric constant is calculated as a function of increasing domain wall density and temperature. We find an increase of dielectric permittivity with increasing domain wall density, which is expected to occur at low driving field where the lateral motion of domain walls is forbidden. Real-space decomposition of dielectric response reveals that frustrated dipoles within the finite width of the domain walls are responsible for the enhanced low-field permittivity.

* sliu@carnegiescience.edu

† rcohen@carnegiescience.edu

Ferroelectrics characterized by the switchable spontaneous polarization under external field have served as critical components in electronics, optics, sensors, and actuators. [1] Ferroelectrics often possess complex domain structures with domain walls separating homogeneously polarized domains. In response to an applied stimulus that favors one polarization state over another, the domain wall can move to increase the size of the favored domain. [2] The susceptibility therefore consists of two contributions: the *intrinsic* contribution that originates from the polarization change within the bulk of the domains and the *extrinsic* contribution that arises from domain wall motions. It is now widely recognized that domain walls can have a profound effect on the dielectric, piezoelectric and pyroelectric susceptibilities of ferroelectric materials. [3–8] For example, experiments suggested that most ($> 60\%$) of the dielectric and piezoelectric responses at room temperature in lead zirconate-titanate (PZT) ceramics is from the domain wall contributions [3, 5], with both 180° and non- 180° walls contributing to dielectric response and non- 180° walls affecting piezoelectricity. [9, 10]

Controllably optimizing the susceptibilities of ferroelectrics through domain wall engineering requires a microscopic understanding of the dynamics of domain walls in response to an stimulus. For a driving field of large amplitude, the domain wall contribution to the susceptibility shows strong field-amplitude dependence, which is attributed to the field-induced irreversible domain wall motion. The upper bound of the dielectric permittivity due to the displacement of 180° domain wall can be approximated as $\epsilon^{\text{DW}} \cong 2P_s/\epsilon_0 E_c$, where P_s is the bulk polarization, E_c is the coercive field and the factor of two comes from polarization reversal. For BaTiO_3 , using $P_s = 0.25 \text{ C/m}^2$ and $E_c = 1\text{kV/cm}$ gives $\epsilon^{\text{DW}} \cong 560,000$. The total dielectric response is the weighted average of domain wall contribution and intrinsic bulk contribution, and is often much smaller than the upper bound due to the low volume fraction of domain wall.

For a stimulus that is much smaller than the coercive field, a number of mechanisms have been proposed to explain domain wall contribution to the enhanced dielectric response in the absence of domain wall motion. [11, 12] Lawless and Fousek proposed that the domain wall has excessive polarizability because the materials within the wall have polarization passing through zero and can be considered as being closer to the phase transition than materials in the bulk. [11] The temperature gradient and heat transfer across domain walls induced by electrocaloric effect of anti-parallel domains was also suggested to affect the frequency dispersion of dielectric susceptibility. [12]

The idea of reversible domain wall vibration was also proposed to explain small-signal response. Unlike the typical domain wall motion that moves from one Peierls potential to another via nucleation-and-growth mechanism, [13] reversible domain wall motion comes from domain wall displacement inside one minimum of the Peierls potential. [14] The domain wall is considered as an oscillator with some effective mass and vibrates around the equilibrium position with displacement amplitude determined by electric and/or elastic restoring forces. [15–20] However, the estimated domain wall displacement is only few percent of a lattice constant [11, 17], which is not well defined microscopically considering that 1) atoms are discrete in crystalline solids; 2) a domain wall is at least one unit cell wide; 3) atoms move *perpendicular* to the direction of the domain wall vibration. Furthermore, the assumption that a domain wall has effective mass directly implies that a domain wall would exhibit inertial response, which was a subject of debate with both confirming [21, 22] and contradicting results [23, 24]. Molecular dynamics simulations of post-field domain wall behavior show that ferroelectric domain walls have no significant intrinsic inertial response. [25] All these results challenge the concept of reversible domain wall vibrations at low field. Recent experiments in (111)-oriented $\text{PbZr}_{0.2}\text{Ti}_{0.8}\text{O}_3$ thin films that effectively freeze out domain wall motions indicate that the stationary contribution from the domain wall can be 6-78 times larger than bulk response [6, 8], but the exact microscopic nature of stationary domain wall contribution remains unclear.

We first explore the structure and static dielectric response of 180° domain wall in PbTiO_3 with first-principles density functional theory within the local-density approximation. The 180° domain wall is modeled with a $12 \times 1 \times 1$ supercell with lattice constants of unit cells fixed to experimental values ($a = 3.9 \text{ \AA}$, $c = 4.15 \text{ \AA}$). Both previous [26] and our *ab initio* calculations have shown that Pb and Ti atoms within the domain wall have smaller atomic displacements (with respect to the center of oxygen cage) than those located in bulk-like domains (Fig. 1a). Accordingly, Pb and Ti atoms at domain walls (@DW in Fig. 1b) have much shallower potential energy surfaces for small distortions away from the equilibrium position. This indicates that atoms within domain walls are easier to move under a driving field.

Next, we investigate the effect of atomic displacement on the value of static dielectric constant of PbTiO_3 with density perturbation functional theory (DPFT) using the ABINIT code. [27] We start with a fully relaxed 5-atom unit cell of PbTiO_3 , and apply small distur-

tions to the Ti (Pb) atom. For each distorted structure, we calculate the short-axis (ε_a) and long-axis (ε_c) dielectric constants. It is found that structures with suppressed Pb and Ti displacement have both larger ε_a and ε_c (Fig. 1c and d). This shows that the domain wall characterized with smaller atomic displacements will possess higher dielectric susceptibility.

To understand the finite-temperature dielectric response of domain walls, we perform all-atom molecular dynamics (MD) simulations taking the ferroelectric 180° domain wall and ferroelastic 90° domain wall in PbTiO₃ as examples. Combined with accurate interatomic potentials derived from *ab initio* calculations [28–30], MD simulations have been applied to study various aspects of ferroelectrics [25, 31–33] in different environments. [34–36] Our force field of PbTiO₃ is developed based on the bond-valence theory and is parametrized from first-principles. [30] All simulations are performed under constant-volume constant-temperature (*NVT*) conditions over a wide range of temperatures (150–320 K) with lattice constants of unit cells fixed to experimental values. To determine the effect of domain wall density on the total dielectric response, the simulations for 180° domain walls are carried out over a $48a \times 8a \times 8c$ perovskite-type supercell with varying numbers (2, 4, 6, 8, 10, 12) of walls under periodic boundary conditions. An $80a_x \times 6a_y \times 80a_z$ supercell is used to model domain structures with 90° walls, where $a_x = (a + c)/2$, $a_y = a$, and $a_z = (a + c)/2$ are averaged lattice constants along Cartesian axes. This choice of supercell dimensions leads to a typical $c/a/c/a$ multidomain structure. [37]

The local static dielectric permittivity(susceptibility) tensor at unit cell m , ε_{ij}^m (χ_{ij}^m), is calculated using [33, 38–40]:

$$\chi_{ij}^m \approx \varepsilon_{ij}^m = \frac{V}{\varepsilon_0 k_B T} \left(\langle P_i^m P_j^m \rangle - \langle P_i^m \rangle \langle P_j^m \rangle \right) \quad (1)$$

where ε_0 is vacuum permittivity, k_B is the Boltzmann constant, T is the temperature, V is the volume of unit cell, i and j define Cartesian components, P_i^m is the local (within the unit cell m) polarization of i th component, and $\langle \dots \rangle$ represents the thermal average. The magnitude of polarization fluctuations dictates the magnitude of dielectric response. The instantaneous local polarization $\mathbf{P}^m(t)$ is

$$\mathbf{P}^m(t) = \frac{1}{V} \left(\frac{1}{8} \mathbf{Z}_{\text{Pb}}^* \sum_{i=1}^8 \mathbf{r}_{\text{Pb},i}^m(t) + \mathbf{Z}_{\text{Ti}}^* \mathbf{r}_{\text{Ti}}^m(t) + \frac{1}{2} \mathbf{Z}_{\text{O}}^* \sum_{i=1}^6 \mathbf{r}_{\text{O},i}^m(t) \right) \quad (2)$$

where \mathbf{Z}_{Pb}^* , \mathbf{Z}_{Ti}^* , and \mathbf{Z}_{O}^* are the Born effective charges of Pb, Ti, and O atoms; $\mathbf{r}_{\text{Pb},i}^m(t)$, $\mathbf{r}_{\text{Ti},i}^m(t)$, and $\mathbf{r}_{\text{O},i}^m(t)$ are instantaneous atomic positions in unit cell m . The total dielectric

response of the supercell is estimated by taking the average of the local dielectric permittivity or local dielectric susceptibility ($1/\epsilon_{ij}^m$), depending on the connection style (parallel vs. serial) of unit cells (approximated as capacitors).

The polarization profiles for domain structures with 180° walls at 300 K obtained from MD simulations reveal frustrated polarization at domain boundaries (Fig. 2). The width of a domain wall is approximately two unit cells thick, consistent with first-principle calculations. Within domain walls, the polarization ($P^{\text{DW}} \approx 0.45 \text{ C/m}^2$) is much smaller than the polarization in adjacent bulk-like domains ($P^{\text{bulk}} \approx 0.8 \text{ C/m}^2$). This is due to the competition between minimizing the local energy, which favors small deviation of local polarization from the bulk value, and minimizing the gradient energy, which prefers a small polarization change, $2P^{\text{DW}}$, across the domain boundary. The dipoles of smaller magnitude are expected to be more susceptible to external stimuli. We consider the dielectric permittivity in response to an electric field applied along the polar axis (z axis), ϵ_{zz} . Figure 3 presents the unit-cell-resolved polarization profile and dielectric permittivity for a supercell with 12 walls. The layers within the domain walls clearly possess higher permittivity (≈ 60), and the layers in the domains have permittivity comparable to single domain value (≈ 30). This is a direct consequence of larger polarization fluctuation associated with smaller dipoles.

We further estimated the total dielectric constant as a function of temperature and the volume fraction (γ) of domain walls. The volume fraction of domain walls is defined as $2n^{\text{DW}}/N$ where n^{DW} is the number of domain walls, $N = 48$ is the supercell dimension along the x axis, and the factor of two comes from the observation that each domain wall consists of two layers of unit cells. We find a nearly linear dependence of ϵ_{zz} on temperature below 350 K, far below the phase transition temperature of PbTiO_3 (Fig. 4a), and ϵ_{zz} increases almost linearly with γ under a given temperature (Fig. 4c).

The real-space decomposition of the total ϵ_{zz} allows the examination of individual contributions from domain walls ($\epsilon_{zz}^{\text{DW}}$) and domains (ϵ_{zz}^{D}), with the total $\epsilon_{zz} = \gamma\epsilon_{zz}^{\text{DW}} + (1 - \gamma)\epsilon_{zz}^{\text{D}}$, as the multidomain configuration can be viewed as a set of parallel capacitors for the response along z . $\epsilon_{zz}^{\text{DW}}$ and ϵ_{zz}^{D} have different temperature dependences (Fig. 4b), with $\epsilon_{zz}^{\text{DW}}$ possessing a stronger temperature dependence (larger $\epsilon_{zz}^{\text{DW}}-T$ slope) than ϵ_{zz}^{D} . Interestingly, a noticeable increase in ϵ_{zz}^{D} with decreasing domain size is observed. In addition, the contribution of domain walls to the total dielectric response, defined as $f^{\text{DW}} = \gamma\epsilon_{zz}^{\text{DW}}/\epsilon_{zz}$, is as high as 50% even for a relatively low domain wall volume fraction ($\gamma \approx 0.35$, Fig. 4d).

These results demonstrate that *even in the absence of domain wall motion*, the stationary 180° domain wall structure itself can enhance the dielectric response by almost a factor of two at room temperature.

Similar susceptibility enhancement applies to 90° walls as well. Figure 5 shows the simulated layer-resolved polarization profiles at 300 K for multidomain structures with 90° walls separating $+P_z$ (green) and $+P_x$ (red) domains. The width of 90° domain walls is 4-5 unit cells, and dipoles within domain walls have smaller magnitudes, just as 180° domain walls. We used an orthorhombic supercell, so the angle between the polarization axes of neighboring domains is exactly 90° instead of $2\arctan(a/c)$ that is geometrically required for a tetragonal ferroelectric. The domains are therefore strained. We find that when the domain size is comparable to the domain wall thickness, the unit cells inside domains also obtain smaller polarization. Here, we focus on the ε_{zz} component in response to electric field along the z direction. The real-space profile of local ε_{zz}^m for a supercell with four walls at 300 K reveals that domain boundaries have larger permittivity values (Fig. 6a). Layer-resolved ε_{zz} (Fig. 6b) provides more details. As expected, the ε_{zz} of P_z domains is smaller than that of P_x domains. This agrees with first-principles [41, 42] and experimental [43, 44] results that PbTiO₃ in the tetragonal phase has a higher dielectric constant along the short axis. The values of local permittivity at 90° domain walls are about two times higher than those in domains. We also note that the ε_{zz} of P_z domains in domain structures with only 90° walls is higher than that in domain structures with only 180° walls (Fig. 3). This is due to the strain effect discussed above, and is consistent with the experimental and theoretical observations that compressive strain gives rise to larger dielectric constant in ferroelectric thin films and superlattices, [45, 46] and is also consistent with our DFT calculations that reduced atomic displacements cause higher dielectric response (Fig. 1c and d). The intrinsic ε_{zz} for a domain structure with 50% a domain and 50% c domain is about 40-60, estimated with $2/(\varepsilon_a^{-1} + \varepsilon_c^{-1})$ assuming c and a domains as serial capacitors. Our simulations show that the domain structure with 90° walls has much larger dielectric response, and more domain walls lead to higher values (Fig. 6c). This highlights the contribution from stationary domain walls. The $\varepsilon_{zz}^{\text{DW}}$ of 90° wall in PbTiO₃ is about 6 times larger than the single domain value. It is noted that for the supercell with 16 walls, we observe domain merger at temperatures above 250 K due to thermal broadening of domain walls: the final domain structure contains only four 90° walls.

The enhanced dielectric constants resulting from smaller dipoles at domain boundaries also have important indications for the nucleation step in ferroelectric switching. The classic Miller-Weinreich (MW) nucleation model [47] for domain wall motion assumes depolarization interactions between boundary charges dominate the nucleation step. To reduce the repulsive energy penalty due to Coulomb repulsions between positive depolarization charges, the MW model incorrectly leads to triangular-shaped nucleus with a small width and large nucleation barrier. [48] The depolarization energy U_d in the MW model depends on P_s^2/ε , where P_s is the bulk polarization as a sharp polarization change from $P_s \rightarrow -P_s$ is assumed. Therefore, the polarization frustration that actually occurs at domain walls should substantially reduce the depolarization energy because of the smaller polarization gradient thus smaller boundary charges and larger dielectric screening. [13] Similar polarization frustration is likely to occur at ferroelectric/metal interface, and may also play a role in resolving the Landauer’s paradox of an implausibly large nucleation energy barrier ($10^8 k_B T$) for single domain switching.

Distinguishing and understanding the origins of various contributions to ferroelectric susceptibility is critical for controlled materials design and performance optimization. Our first-principles and molecular dynamics simulations demonstrate that the frustrated dipoles within the domain walls acquire larger dipole fluctuation and are responsible for the enhanced dielectric response of stationary domain walls under subswitching field. Our work suggests that the dielectric constant at the domain wall can be two times higher than defect-free bulk. The mechanism applies to *all* types of domain walls, as polarization suppression at domain boundaries is the natural consequence of reducing gradient energy penalty. Exploring how defect pinning of domain wall may influence the stationary domain wall contribution will be a useful future research.

Acknowledgements This work is partly supported by US ONR. SL and REC are supported by the Carnegie Institution for Science. REC is also supported by the ERC Advanced Grant ToMCaT. Computational support was provided by the US DOD through a Challenge Grant from the HPCMO.

- [1] J. F. Scott, *Science* **315**, 954 (2007).
- [2] A. Pramanick, A. D. Prewitt, J. S. Forrester, and J. L. Jones, *Crit. Rev. Solid State Mater. Sci.* **37**, 243 (2012).
- [3] Q. Zhang, H. Wang, N. Kim, and L. Cross, *J. Appl. Phys.* **75**, 454 (1994).
- [4] D. Taylor and D. Damjanovic, *J. Appl. Phys.* **82**, 1973 (1997).
- [5] F. Xu, S. Trolier-McKinstry, W. Ren, B. Xu, Z.-L. Xie, and K. Hemker, *J. Appl. Phys.* **89**, 1336 (2001).
- [6] R. Xu, J. Karthik, A. R. Damodaran, and L. W. Martin, *Nat. Comm.* **5**, 3120 (2014).
- [7] J. Karthik and L. Martin, *Phys. Rev. B* **84**, 024102 (2011).
- [8] J. Karthik, A. Damodaran, and L. Martin, *Phys. Rev. Lett.* **108**, 167601 (2012).
- [9] A. Pramanick, D. Damjanovic, J. E. Daniels, J. C. Nino, and J. L. Jones, *Journal of the American Ceramic Society* **94**, 293 (2011).
- [10] R. J. Zednik, A. Varatharajan, M. Oliver, N. Valanoor, and P. C. McIntyre, *Adv. Funct. Mater.* **21**, 3104 (2011).
- [11] W. N. Lawless and J. Fousek, *Journal of the Physical Society of Japan* **28**, 419 (1970).
- [12] M. Marvan, *Czechoslovak Journal of Physics* **19**, 482 (1969).
- [13] S. Liu, I. Grinberg, and A. M. Rappe, *Nature* **534**, 360 (2016).
- [14] A. K. Tagantsev, L. E. Cross, and J. Fousek, *Domains in Ferroic Crystals and Thin Films* (Springer, 2010).
- [15] C. Kittel, *Phys. Rev.* **83**, 458 (1951).
- [16] J. Fousek and B. Brezina, *J. Phys. Soc. Jpn.* **19**, 830 (1964).
- [17] G. Arlt, H. Dederichs, and R. Herbiet, *Ferroelectrics* **74**, 37 (1987).
- [18] G. Arlt and N. A. Pertsev, *J. Appl. Phys.* **70**, 2283 (1991).
- [19] N. A. Pertsev, G. Arlt, and A. G. Zembilgotov, *Microelectron. Eng.* **29**, 135 (1995).
- [20] N. A. Pertsev, G. Arlt, and A. G. Zembilgotov, *Phys. Rev. Lett.* **76**, 1364 (1996).

- [21] Y. Kim, H. Han, W. Lee, S. Baik, D. Hesse, and M. Alexe, Nano Lett. **10**, 1266 (2010).
- [22] M. Dawber, D. J. Jung, and J. F. Scott, Appl. Phys. Lett. **82**, 436 (2003).
- [23] P. Sharma, R. G. P. McQuaid, L. J. McGilly, J. M. Gregg, and A. Gruverman, Adv. Mater. **25**, 1323 (2013).
- [24] M. Molotskii, Y. Rosenwaks, and G. Rosenman, Annu. Rev. Mater. Res. **37**, 271 (2007).
- [25] S. Liu, I. Grinberg, and A. M. Rappe, Appl. Phys. Lett. **103**, 232907 (2013).
- [26] B. Meyer and D. Vanderbilt, Phys. Rev. B **65**, 104111 (2002).
- [27] X. Gonze, B. Amadon, P.-M. Anglade, J.-M. Beuken, F. Bottin, P. Boulanger, F. Bruneval, D. Caliste, R. Caracas, M. Cote, T. Deutsch, L. Genovese, P. Ghosez, M. Giantomassi, S. Goedecker, D. Hamann, P. Hermet, F. Jollet, G. Jomard, S. Leroux, M. Mancini, S. Mazevet, M. Oliveira, G. Onida, Y. Pouillon, T. Rangel, G.-M. Rignanese, D. Sangalli, R. Shaltaf, M. Torrent, M. Verstraete, G. Zerah, J. Z. X. Gonze, B. Amadon, P.-M. Anglade, J.-M. Beuken, F. Bottin, P. Boulanger, F. B. and' D. Caliste, R. Caracas, M. Cote, T. Deutsch, L. Genovese, P. Ghosez, M. Giantomassi, S. Goedecker, D. Hamann, P. Hermet, F. Jollet, G. Jomard, S. Leroux, M. Mancini, S. Mazevet, M. Oliveira, G. Onida, Y. Pouillon, T. Rangel, G.-M. Rignanese, D. Sangalli, R. Shaltaf, M. Torrent, M. Verstraete, G. Zerah, J. Z. X. Gonze, B. Amadon, P.-M. Anglade, J.-M. Beuken, F. Bottin, P. Boulanger, F. B. and' D. Caliste, R. Caracas, M. Cote, T. Deutsch, L. Genovese, P. Ghosez, M. Giantomassi, S. Goedecker, D. Hamann, P. Hermet, F. Jollet, G. Jomard, S. Leroux, M. Mancini, S. Mazevet, M. Oliveira, G. Onida, Y. Pouillon, T. Rangel, G.-M. Rignanese, D. Sangalli, R. Shaltaf, M. Torrent, M. Verstraete, G. Zerah, and J. Zwanziger, Computer Phys. Commun. **180**, 2582 (2009).
- [28] M. Sepliarsky and R. E. Cohen, AIP Conf. Proc. **626**, 36 (2002).
- [29] M. Sepliarsky and R. E. Cohen, Journal of Physics: Condensed Matter **23**, 435902 (2011).
- [30] S. Liu, I. Grinberg, and A. M. Rappe, J. Physics.: Condens. Matter **25**, 102202 (2013).
- [31] M. C. Rose and R. E. Cohen, Phys. Rev. Lett. **109**, 187604 (2012).
- [32] X. Zeng and R. E. Cohen, Appl. Phys. Lett. **99**, 142902 (2011).
- [33] T. Hashimoto and H. Moriwake, Molecular Simulation **41**, 1074 (2014).
- [34] M. Sepliarsky, M. G. Stachiotti, and R. L. Migoni, Phys. Rev. B **72**, 014110 (2005).
- [35] R. Xu, S. Liu, I. Grinberg, J. Karthik, A. R. Damodaran, A. M. Rappe, and L. W. Martin, Nat. Mater. **14**, 79 (2015).
- [36] I. G. Hiroyuki Takenaka and A. M. Rappe, Phys. Rev. Lett. **110**, 147602 (2013).

- [37] N. A. Pertsev and A. G. Zembilgotov, J. Appl. Phys. **80**, 6401 (1996).
- [38] S. H. Wemple, M. DiDomenico, and A. Jayaraman, Phys. Rev. **180**, 547 (1969).
- [39] S. Boresch, P. Höchtl, and O. Steinhauser, J. Phys. Chem. B **104**, 8743 (2000).
- [40] I. Ponomareva, L. Bellaiche, T. Ostapchuk, J. Hlinka, and J. Petzelt, Phys. Rev. B **77**, 012102 (2008).
- [41] L. Yu, V. Ranjan, M. B. Nardelli, and J. Bernholc, Phys. Rev. B **80**, 165432 (2009).
- [42] G. Pilania and R. Ramprasad, J Mater Sci **47**, 7580 (2012).
- [43] C. M. Foster, Z. Li, M. Grimsditch, S.-K. Chan, and D. J. Lam, Phys. Rev. B **48**, 10160 (1993).
- [44] M. D. Fontana, H. Idrissi, G. E. Kugel, and K. Wojcik, J. Phys.: Condens. Matter **3**, 8695 (1991).
- [45] C. Bungaro and K. M. Rabe, Phys. Rev. B **69**, 184101 (2004).
- [46] B. H. Park, E. J. Peterson, Q. X. Jia, J. Lee, X. Zeng, W. Si, and X. X. Xi, Appl. Phys. Lett. **78**, 533 (2001).
- [47] R. C. Miller and G. Weinreich, Phys. Rev. **117**, 1460 (1960).
- [48] T. Tybell, P. Paruch, T. Giamarchi, and J.-M. Triscone, Phys. Rev. Lett. **89**, 097601 (2002).

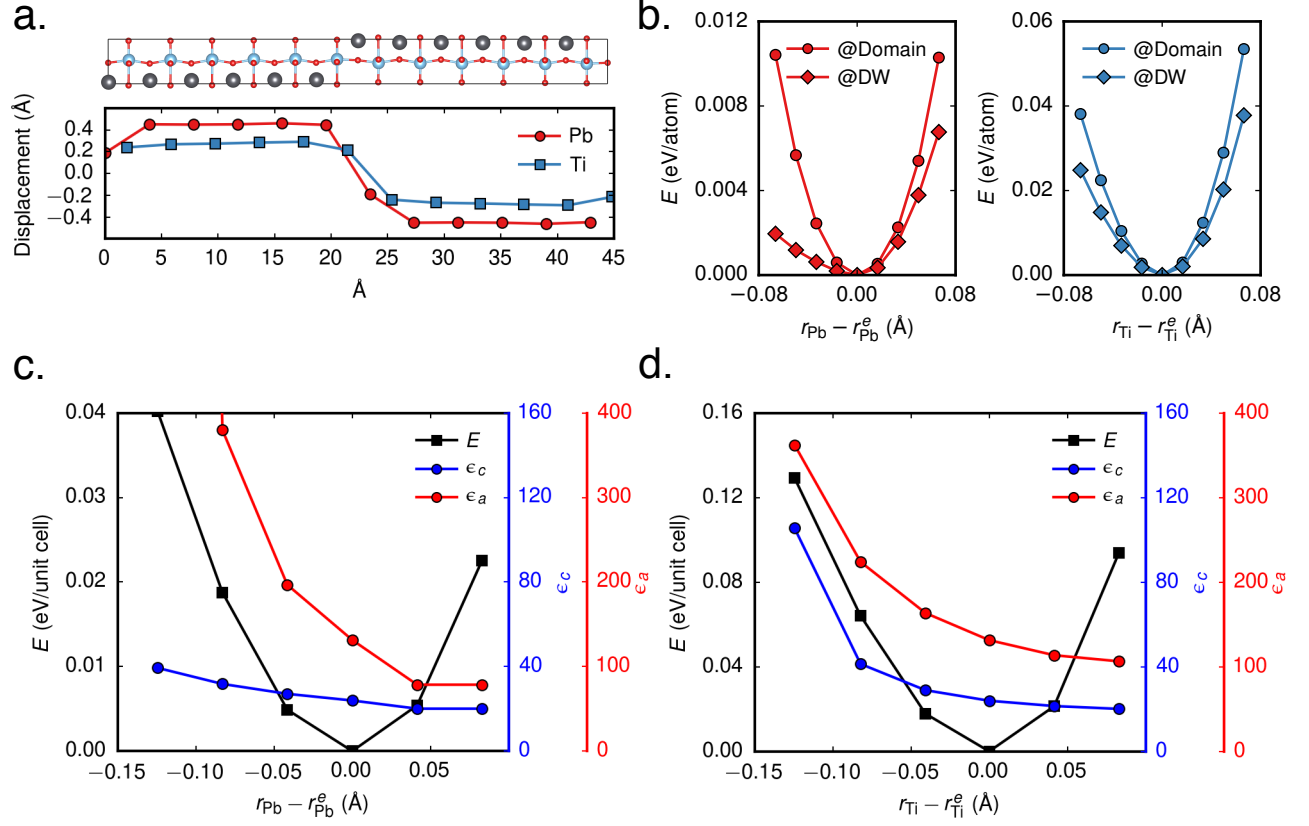


FIG. 1. First-principles modeling of 180° domain walls in PbTiO₃. (a) z displacement of Ti and Pb atoms relative to the center of oxygen cage. (b) Potential energy surfaces for Pb and Ti atoms at domain walls (@DW) and in the bulk (@Domain). Energy and dielectric constants of 5-atom unit cell of PbTiO₃ as a function of atomic distortion along the polar axis for Pb (c) and Ti (d).

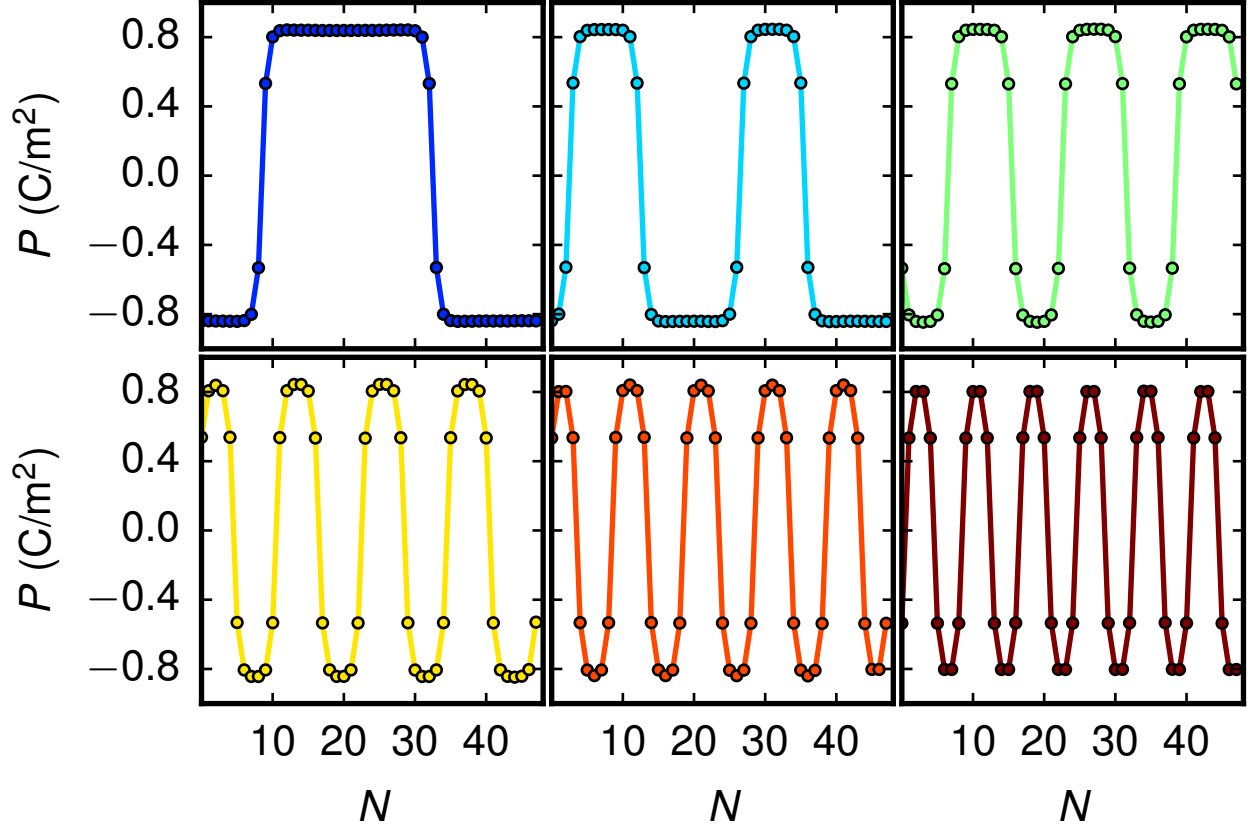


FIG. 2. Simulated layer-resolved polarization profiles for supercells with 2, 4, 6, 8, 10, and 12 domain walls with a $48 \times 8 \times 8$ supercell. The layer in y - z plane is indexed along the x axis. The layers at domain boundaries have smaller polarizations.

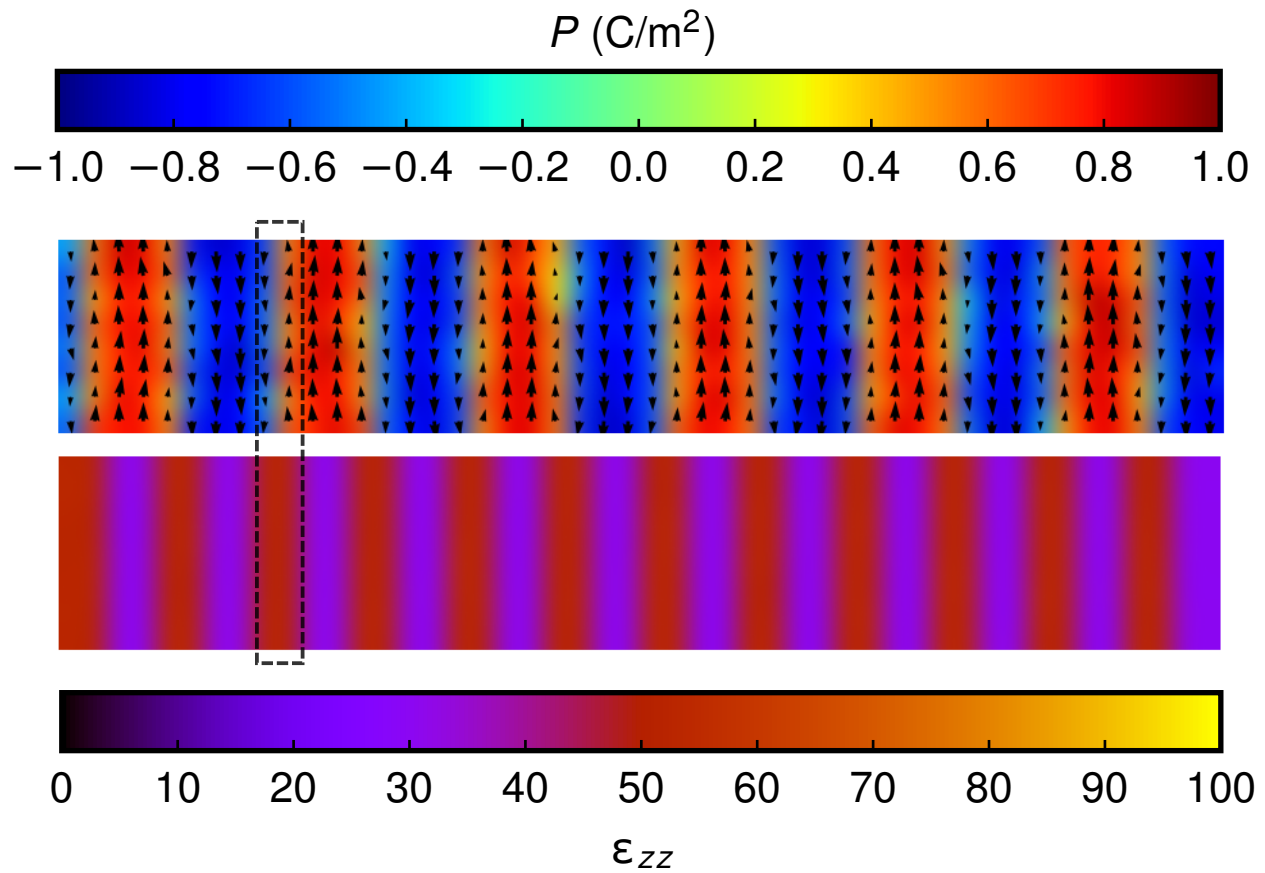


FIG. 3. Profiles for local polarization P_z^m (top) and local ϵ_{zz}^m (bottom). The black arrows represent local dipoles. The position of one domain wall is highlight by the dashed rectangle.

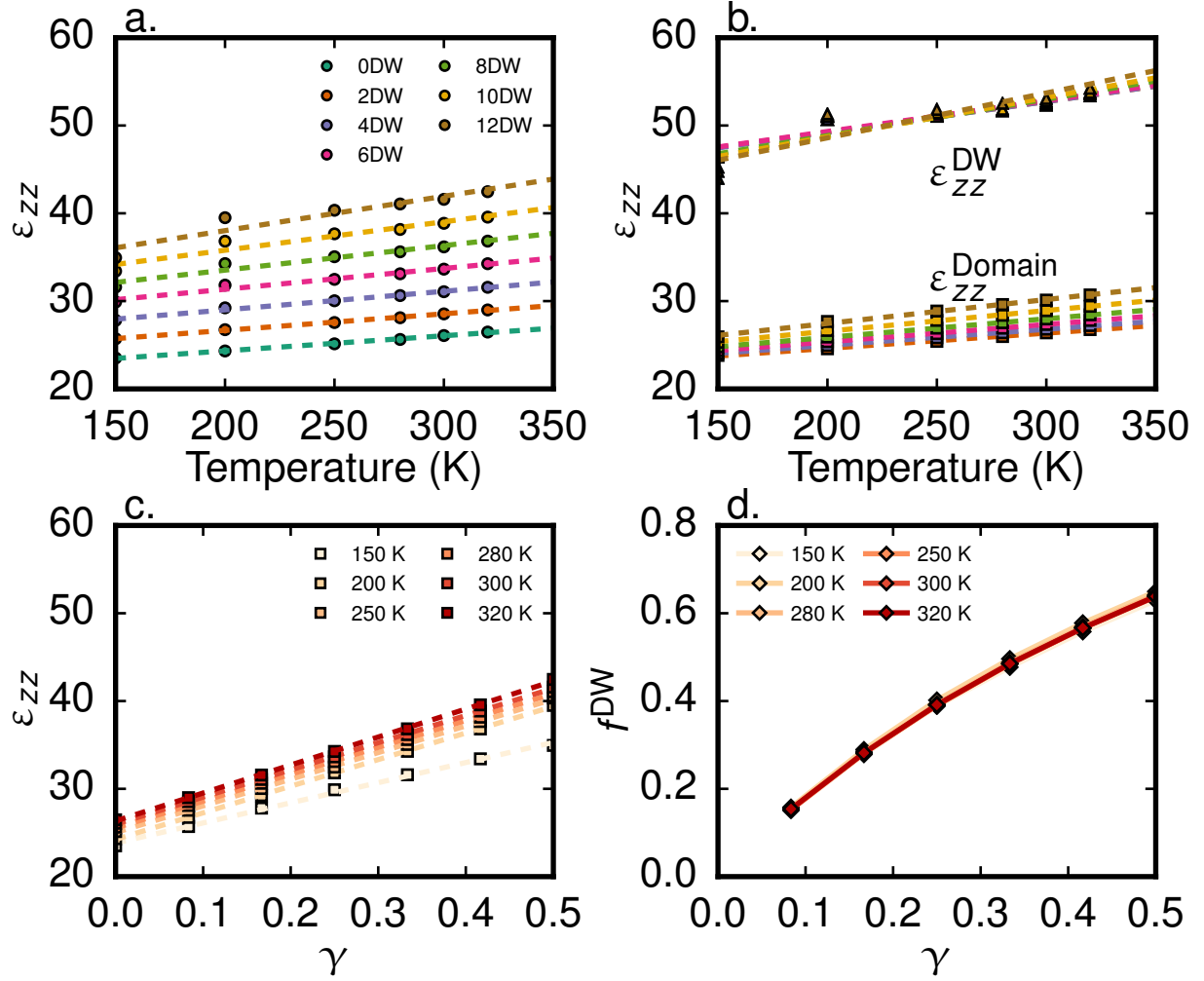


FIG. 4. Temperature dependence of (a) total dielectric constant ϵ_{zz} and (b) domain wall dielectric constant ϵ_{zz}^{DW} and domain dielectric constant ϵ_{zz}^D for supercells containing different number of 180° walls. Domain wall volume fraction (γ) dependence of (c) total dielectric constant ϵ_{zz} under different temperatures and (d) the weight of domain wall contribution (f^{DW}).

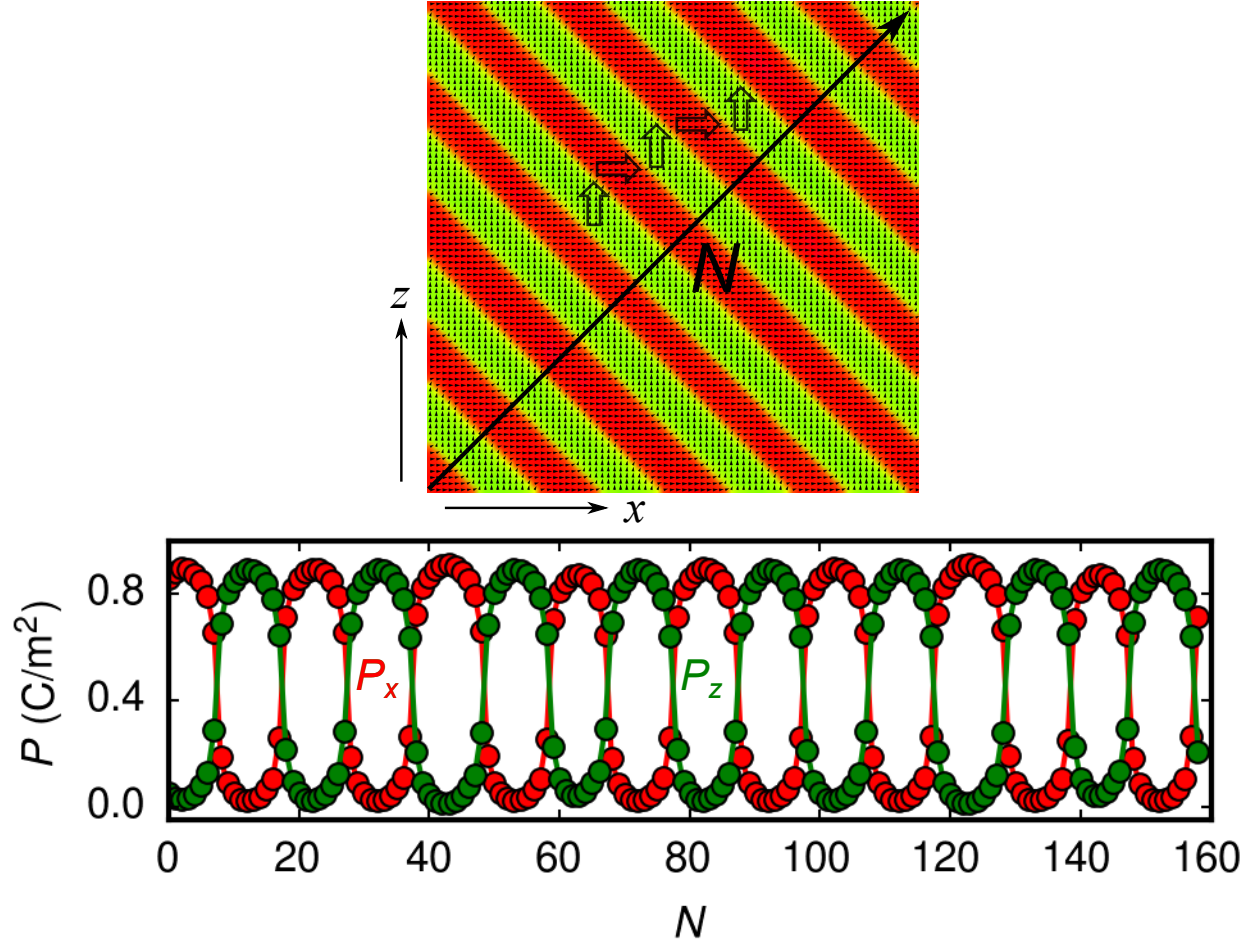


FIG. 5. Molecular dynamics simulations of 90° domain walls. The zig-zag domain pattern (top) with 90° domain walls separating P_x (red) domains and P_z (green) domains. Layer-resolved x -component and z -component polarization profile (bottom) for supercells with 16 walls. The layer is indexed along $[110]$ direction.

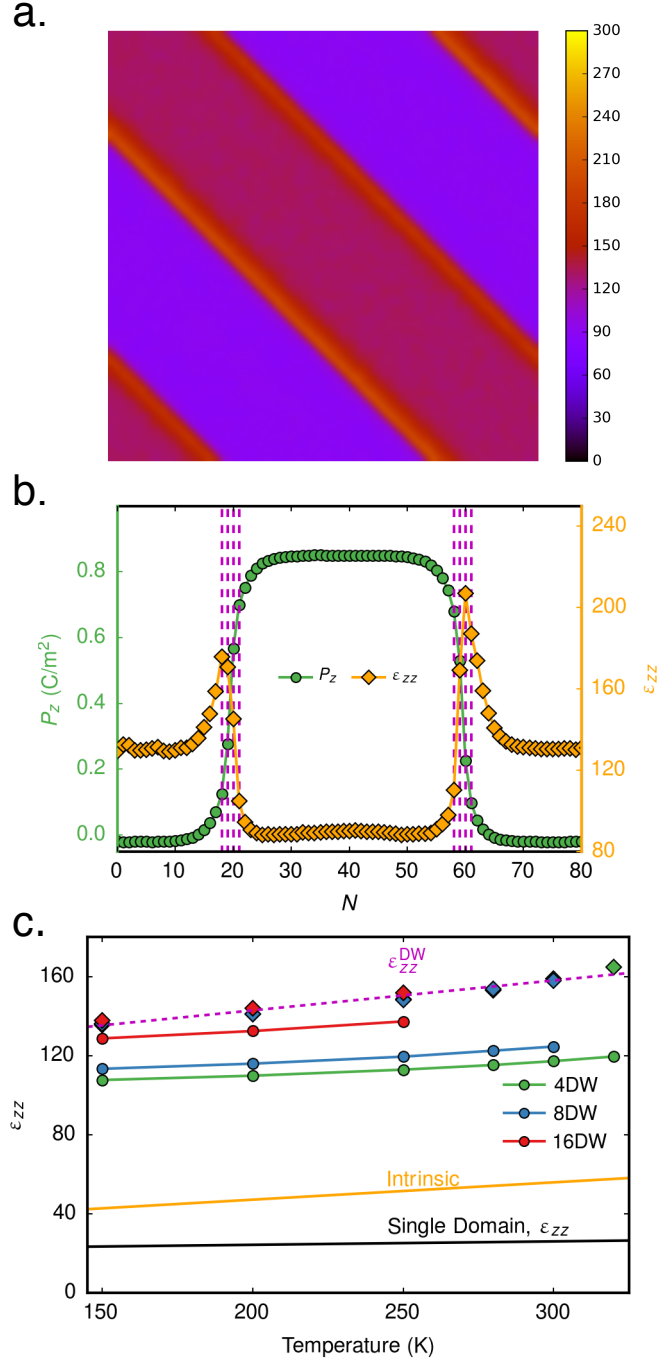


FIG. 6. (a) Profile of local $\epsilon_{zz}^{\text{DW}}$ for a supercell with four 90° walls at 300 K. (b) Layer-resolved polarization profiles and ϵ_{zz} . Only half of the supercell is shown. Temperature dependence of (c) total ϵ_{zz} (circle) and (d) domain wall dielectric constant $\epsilon_{zz}^{\text{DW}}$ (square) for supercells containing different numbers of 90° walls.